

glasses of various kinds. Finally, we note that the very slow  $\log(t)$  long-time aging of the storage modulus is reminiscent of similar stretched dynamics in systems with quenched (9) or self-induced (26, 28) disorder.

### References and Notes

- E. M. Herzig, K. A. White, A. B. Schofield, W. C. K. Poon, P. S. Clegg, *Nat. Mater.* **6**, 966 (2007).
- P. Poulin, H. Stark, T. C. Lubensky, D. A. Weitz, *Science* **275**, 1770 (1997).
- U. Tkalec, M. Ravnik, S. Čopar, S. Žumer, I. Mušević, *Science* **333**, 62 (2011).
- P. G. de Gennes, J. Prost, *The Physics of Liquid Crystals* (Oxford Univ. Press, Oxford, 1995).
- S. K. Pal, A. Agarwal, N. L. Abbott, *Small* **5**, 2589 (2009).
- A. Agarwal, E. Huang, S. Palecek, N. L. Abbott, *Adv. Mater.* **20**, 4804 (2008).
- S. J. Woltman, G. D. Jay, G. P. Crawford, *Nat. Mater.* **6**, 929 (2007).
- T. Araki, M. Buscaglia, T. Bellini, H. Tanaka, *Nat. Mater.* **10**, 303 (2011).
- E. H. Brandt, *Rep. Prog. Phys.* **58**, 1465 (1995).
- M. J. Bowick, L. Chandar, E. A. Schiff, A. M. Srivastava, *Science* **263**, 943 (1994).
- H. Stark, *Phys. Rep.* **351**, 387 (2001).
- R. W. Ruhwandl, E. M. Terentjev, *Phys. Rev. E* **55**, 2958 (1997).
- I. Mušević, M. Škarabot, *Soft Matter* **4**, 195 (2008).
- O. Guzmán, E. B. Kim, S. Grollau, N. L. Abbott, J. J. de Pablo, *Phys. Rev. Lett.* **91**, 235507 (2003).
- T. Araki, H. Tanaka, *Phys. Rev. Lett.* **97**, 127801 (2006).
- M. Ravnik et al., *Phys. Rev. Lett.* **99**, 247801 (2007).
- V. J. Anderson, E. M. Terentjev, S. P. Meeker, J. Crain, W. C. K. Poon, *Eur. Phys. J. E* **4**, 11 (2001).
- A. G. Chmielewski, E. Lepakiewicz, *Rheol. Acta* **23**, 207 (1984).
- A. Mertelj, M. Čopič, *Phys. Rev. E* **69**, 021711 (2004).
- L. M. Walker, N. J. Wagner, R. G. Larson, P. A. Mirau, P. Moldenaers, *J. Rheol.* **39**, 925 (1995).
- J. D. Bunning, T. E. Faber, P. L. Sherrell, *J. Phys.* **42**, 1175 (1981).
- L. Benguigui, *Phys. Rev. Lett.* **53**, 2028 (1984).
- M. Zapotocky, L. Ramos, P. Poulin, T. C. Lubensky, D. A. Weitz, *Science* **283**, 209 (1999).
- N. Osterman, J. Kotar, E. M. Terentjev, P. Cicuta, *Phys. Rev. E* **81**, 061701 (2010).
- A. J. Bray, *Adv. Phys.* **43**, 357 (1994).
- J. Török, S. Krishnamurthy, J. Kertész, S. Roux, *Eur. Phys. J. B* **18**, 697 (2000).
- K. Stratford, R. Adhikari, I. Pagonabarraga, J.-C. Desplat, M. E. Cates, *Science* **309**, 2198 (2005).
- L. F. Cugliandolo, J. Kurchan, R. Monasson, G. Parisi, *J. Phys. A* **29**, 1347 (1996).
- L. Berthier, G. Biroli, *Rev. Mod. Phys.* **83**, 587 (2011).

**Acknowledgments:** The work was funded by Engineering and Physical Sciences Research Council grants EP/D071070/1 and EP/E030173/1. We thank R. Besseling and M. Cates for illuminating discussions.

### Supporting Online Material

www.sciencemag.org/cgi/content/full/334/6052/79/DC1

Materials and Methods

SOM Text

Figs. S1 to S4

References (30–38)

17 June 2011; accepted 24 August 2011

10.1126/science.1209997

# Adaptation to Climate Across the *Arabidopsis thaliana* Genome

Angela M. Hancock,<sup>1</sup> Benjamin Brachi,<sup>2</sup> Nathalie Faure,<sup>2</sup> Matthew W. Horton,<sup>1</sup> Lucien B. Jarymowycz,<sup>1</sup> F. Gianluca Sperone,<sup>1</sup> Chris Toomajian,<sup>3</sup> Fabrice Roux,<sup>2</sup> Joy Bergelson<sup>1\*</sup>

Understanding the genetic bases and modes of adaptation to current climatic conditions is essential to accurately predict responses to future environmental change. We conducted a genome-wide scan to identify climate-adaptive genetic loci and pathways in the plant *Arabidopsis thaliana*. Amino acid-changing variants were significantly enriched among the loci strongly correlated with climate, suggesting that our scan effectively detects adaptive alleles. Moreover, from our results, we successfully predicted relative fitness among a set of geographically diverse *A. thaliana* accessions when grown together in a common environment. Our results provide a set of candidates for dissecting the molecular bases of climate adaptations, as well as insights about the prevalence of selective sweeps, which has implications for predicting the rate of adaptation.

Climate change has already led to altered distributions of species, phenotypic variation, and allele frequencies (1–5), and the impact of changing climates is expected to intensify. The capacity to respond to changing

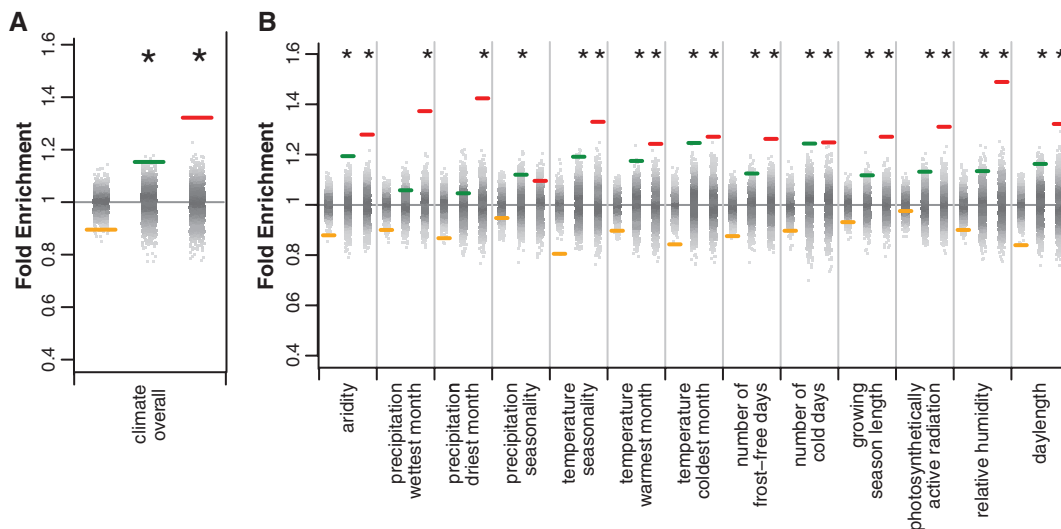
climate is likely to vary widely as a consequence of variation among species in their degree of phenotypic plasticity and their potential for genetic adaptation (6), which in turn depends on the amount of standing genetic variation and the rate

at which new genetic variation arises. *Arabidopsis thaliana* is an excellent model for investigating the genetic basis and mode of adaptation to climate owing to the extensive climatic variation across its native range, as well as the availability of genome-wide single-nucleotide polymorphism (SNP) data among a geographically diverse collection. We examined the correlations between 107 ecologically important phenotypes in *A. thaliana* (7) and 13 climate variables that represent extremes and seasonality of temperature and precipitation, photosynthetically active radiation (PAR), relative humidity, season lengths, and aridity (figs. S1 to S4). We observed strong correlations between

<sup>1</sup>Department of Ecology and Evolution, University of Chicago, 1101 East 57th Street, Chicago, IL 60637, USA. <sup>2</sup>Laboratoire Génétique et Evolution des Populations Végétales, FRE CNRS 3268, Université des Sciences et Technologies de Lille 1, Villeneuve d'Ascq, France. <sup>3</sup>Department of Plant Pathology, Kansas State University, Manhattan, KS 66502, USA.

\*To whom correspondence should be addressed. E-mail: jbergels@uchicago.edu

**Fig. 1.** Enrichment of amino acid-changing SNPs (red), synonymous SNPs (green), and intergenic SNPs (yellow) in the 1% tails of the distributions for (A) climate overall (using a rank statistic based on the minimum rank across climate variables) and (B) for each individual climate variable. Enrichments shown are relative to the proportion of each class of SNPs in the genome overall. Gray dots show the distribution of results of 1000 permutations. The gray line shows the expected enrichment under the null hypothesis of no enrichment. Enrichments that are significant relative to permutations are denoted by asterisks.



day length and phenotypes related to development time and flowering, supporting the observation that flowering time in the field is modulated by complex environmental cues that are difficult to simulate under controlled growth conditions (8–10). Correlations were also found between leaf yellowing (chlorosis) and temperature (11), as well as between dormancy-related traits and those related to temperature and moisture (12), consistent with the role for both vernalization and moisture in breaking dormancy. These results provide evidence for a genetic basis for climate adaptations in *A. thaliana*.

We conducted genome-wide scans to detect climate associations for ~215,000 SNPs genotyped across 948 *A. thaliana* accessions distributed throughout the native range of the species (fig. S5) (13). Because we cannot be certain that our model completely accounts for the effects of population history (13), we tested whether our results detect true signals of adaptations by assessing enrichment of likely functional [i.e., non-synonymous (NS)] variants relative to putative neutrally evolving [i.e., synonymous (S) and intergenic] variants in the 1% tail of the combined climate correlation distributions (14). We found that intergenic SNPs show deficits and NS SNPs show strong and significant enrichments in the tail relative to their proportions in the genome as a whole for climate overall (Fig. 1A), as well as for all but 1 of the 13 individual climate variables (precipitation seasonality; Fig. 1B). The pattern was similar when we controlled for allele frequency but contrasts sharply to climate correlations that did not control for population history (13) (fig. S6).

Notably, for climate overall and for many individual variables, S variants are also significantly enriched in the tail (Fig. 1). The tendency toward enrichment of S variants is expected because of linkage disequilibrium under neutral processes but may be intensified by background selection (15) and/or hitchhiking (16). NS SNPs were slightly enriched relative to S SNPs (ratio of NS to S = 1.146,  $P = 0.036$ ) for climate overall. In addition, precipitation in the wettest and driest months, relative humidity, length of the growing season, and PAR were enriched for NS relative to S variants (ratios ranging from 1.137 to 1.361 and  $P$  values ranging from 0.025 to  $1 \times 10^{-4}$ ). Given that we do not have data for all individual SNPs, but rather use SNPs to represent variation in the genome, these results are surprisingly strong.

We examined which biological processes are overrepresented among strong climate correlations, focusing in particular on climate variables for which we observed a significant NS-to-S enrichment (Table 1 and table S2). PAR shows the largest number of enriched categories, including photosynthesis, auxin biosynthesis, and gravitropism. In addition, we found enrichment of processes related to energy metabolism (i.e., starch metabolism and mitochondrial electron transport) with both precipitation extremes. These links between

energy metabolism and water availability likely result from variation in photosynthetic capacity across precipitation gradients due to differences in the proportion of time when stomata are open (17).

Although pleiotropic gene functions may influence the rate of adaptation (18, 19), we have an incomplete understanding of the extent and magnitude of their effects on adaptation (20). We find substantial overlap in the 1% tails of climate variables, with pairwise combinations sharing 0 to 70% of top SNPs (fig. S7), suggesting that pleiotropy is common among adaptive alleles. However, some of these results may be due to correlations among the climate variables themselves, rather than pleiotropy per se. Indeed, a significant positive correlation was observed between the matrix of pairwise correlation coefficients among climate variables and the matrix of their proportional overlap of SNPs (Mantel  $r^2 = 0.59$ ,  $P = 2 \times 10^{-4}$ ). Hence, outliers that are compared to the variable correlation matrix are particularly interesting (e.g., fig. S8).

It would be difficult to confirm the candidates from climate-related genome scans, even if it were possible to predict climate with absolute certainty, because of the scale of such tests. We thus validated our model by reasoning that if we are observing true signals, then they should be able to predict the relative fitness of genotypes grown in a particular climate. We tested our ability to predict the relative fitness of 147 *A. thaliana* accessions planted in the fall in a common garden in Lille, France (Fig. 2A). In particular, we selected all SNPs in the 0.01% tail of correlations with any climate variable and pruned this set of SNPs to include only one per chromosomal region on the basis of patterns of linkage disequilibrium. We identified alleles that are more common within a window of climate similar to Lille's. Then, we asked whether the count of these alleles could predict relative fitness, as measured by total silique length (21) among the accessions. We created a null distribution by conducting the same analysis on resampled sets of SNPs. We found a strong and significant corre-

**Table 1.** Enrichment of biological processes (BPs) in the 1% tail ( $P < 1 \times 10^{-3}$ ) for climate variables with significant NS relative to S enrichments.

Biological process	Enrichment	P value
<i>Photosynthetically active radiation</i>		
Maintenance of root meristem identity	31.42	$1.0 \times 10^{-5*}$
Indoleacetic acid biosynthetic process	28.94	$1.0 \times 10^{-5*}$
Cellular response to water deprivation	27.26	$6.0 \times 10^{-5*}$
Regulation of defense response	24.24	$2.8 \times 10^{-4}$
Gynoecium development	22.44	$2.0 \times 10^{-5*}$
Red light signaling pathway	21.62	$1.1 \times 10^{-4}$
Stomatal complex development	21.62	$1.1 \times 10^{-4}$
Cotyledon vascular tissue pattern formation	18.96	$5.0 \times 10^{-5*}$
Positive gravitropism	15.47	$1.0 \times 10^{-5*}$
Cotyledon development	10.34	$2.1 \times 10^{-4}$
Phloem or xylem histogenesis	9.09	$3.1 \times 10^{-4}$
Jasmonic acid mediated signaling pathway	7.57	$1.0 \times 10^{-3}$
Photosynthesis	4.59	$1.0 \times 10^{-3}$
Response to cold	2.98	$6.9 \times 10^{-4}$
<i>Precipitation in the wettest month</i>		
Pyridine nucleotide biosynthetic process	17.39	$6.8 \times 10^{-4}$
Base-excision repair	13.59	$9.0 \times 10^{-5}$
Root hair cell tip growth	11.68	$1.0 \times 10^{-3}$
Stomatal complex morphogenesis	11.11	$7.4 \times 10^{-4}$
Starch metabolic process	9.72	$1.0 \times 10^{-3}$
Protein catabolic process	6.42	$2.9 \times 10^{-4}$
Cell division	5.75	$3.0 \times 10^{-4}$
<i>Precipitation in the driest month</i>		
Maintenance of root meristem identity	22.85	$3.6 \times 10^{-4}$
Indoleacetic acid biosynthetic process	21.05	$1.0 \times 10^{-4}$
Mitochondrial electron transport, succinate to ubiquinone	20.68	$1.0 \times 10^{-3}$
<i>Length of the growing season</i>		
Mitochondrial electron transport, NADH to ubiquinone	24.99	$5.0 \times 10^{-4}$
Base-excision repair	13.59	$8.0 \times 10^{-5}$
Epidermal cell differentiation	13.11	$3.0 \times 10^{-4}$
Embryonic development ending in seed dormancy	2.25	$2.2 \times 10^{-4}$
<i>Relative humidity</i>		
Synapsis	12.30	$5.0 \times 10^{-4}$
Regulation of signal transduction	29.99	$1.0 \times 10^{-3}$

\*Significance with  $P < 0.05$  with Bonferroni correction across BP categories ( $P < 6.83 \times 10^{-5}$ ).

lation between the number of favored alleles and fitness (Spearman's  $\rho = 0.48$ ,  $P = 0.003$ ; Fig. 2, B and C), demonstrating that our climate scan is picking up a true signal. As no accessions from within 100 km of Lille were included in the analysis, the correlation between relative fitness and the number of favorable alleles is robust to home versus away effects. Further, additional analyses support this conclusion (13).

The geographic extent of climate-correlated SNPs provides at least an initial picture of how climate shapes patterns of genetic variation in

*A. thaliana*. Geographic extents varied widely across climate variables, with day length and relative humidity representing the extremes (Fig. 3A); SNPs correlated with day length tended to be localized, whereas SNPs correlated with relative humidity tended to be widespread (Fig. 3B and fig. S9). These results, at least in part, can be understood in relation to the geographic distribution of the climate variables themselves.

Narrow SNP distributions may correspond to "hard selective sweeps," or situations in which a new variant was driven quickly to high frequen-

cy in the population. A scan for hard selective sweeps based on extended pairwise haplotype homozygosity (PHS) (22) identified partial selective sweeps throughout the genome and examined the geographic extents of these genomic regions (Fig. 3A). SNPs identified as candidates for selective sweeps were, indeed, shifted toward narrow geographic distributions, consistent with the idea that hard sweeps result in narrow geographic distributions. To quantify the generality of these results, we examined overlap between the 1% tails of the overall climate correlation distributions

**Fig. 2.** The SNPs with strongest climate correlations predict ranks in reproductive success (fitness) in Lille, France. (A) Red dots show the locations where accessions included in the experiment were collected, and the green cross shows the location where plants were grown. (B) The relation between total silique length (a measure of reproductive success) and the number of alleles expected to be favorable based on the climate analysis. (C) Observed Spearman correlation coefficient between total silique length and number of favorable alleles (red line) compared to the distribution of correlation coefficients from permutations.

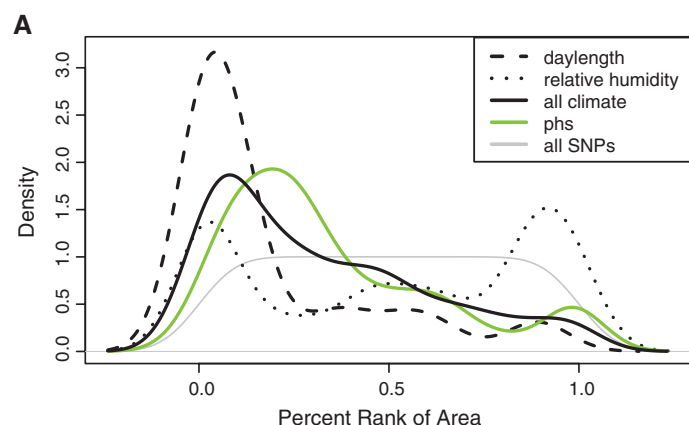
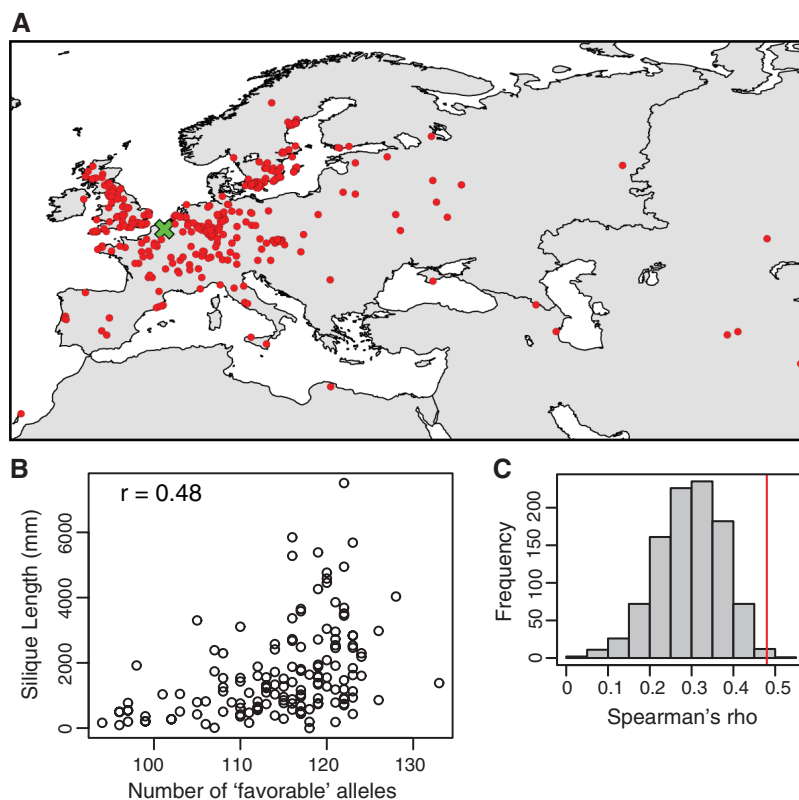
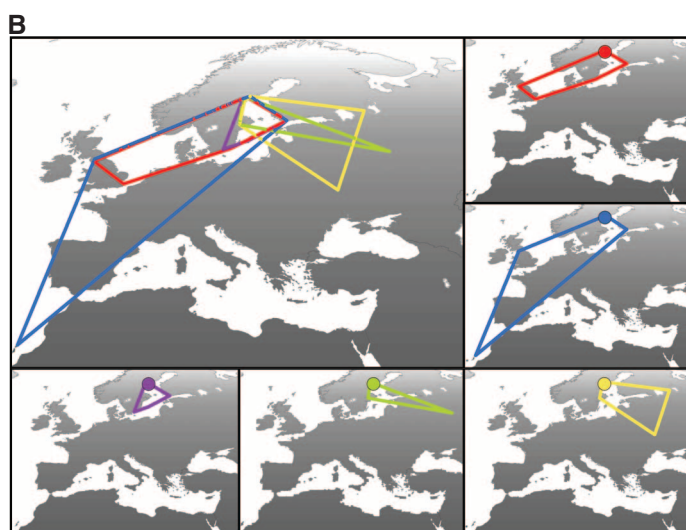


**Fig. 3.** Geographic distributions of SNPs with the strongest climate correlations. (A) Distributions of SNP extents for all SNPs and for SNPs in the 1% tail for climate overall, day length, relative humidity, and PHS. SNPs represented in the plot were filtered to remove redundant information resulting from linkage disequilibrium between SNPs. (B) Distributions of the top five regions for day length overlaid on a map of the distribution of this variable (with values ranging from 12.3 to 16.6 hours). The central panel contains polygons showing the geographic extents of all five SNPs, and other panels show the central feature and extent of each individual SNP.





and the PHS results and found overlap threefold greater than expected by chance if the two variables were independent. This increased to nearly 10-fold enrichment when we examined overlap among the 10% of climate-related SNPs with the smallest geographic extents; enrichments were strongest for aridity, maximum temperature, precipitation in the driest month, and length of the growing season. Although selection on standing variation also plays a role, these results reveal that selective sweeps are likely an important mode of adaptation in *A. thaliana*. The central role of selective sweeps here suggests that species like *A. thaliana* may reach adaptive limits under rapid climate change, owing to the constraints imposed by waiting for new mutations.

## References and Notes

- W. E. Bradshaw, C. M. Holzapfel, *Proc. Natl. Acad. Sci. U.S.A.* **98**, 14509 (2001).
- S. J. Franks, S. Sim, A. E. Weis, *Proc. Natl. Acad. Sci. U.S.A.* **104**, 1278 (2007).
- D. B. Lobell, W. Schlenker, J. Costa-Roberts, *Science* **333**, 616 (2011).
- M. Lynch, R. Lande, in *Biotic Interactions and Global Change*, P. M. Kareiva, J. G. Kingsolver, R. B. Huey,

- (Sinauer Associates, Sunderland, MA, 1993), pp. 234–250.
- P. A. Umina, A. R. Weeks, M. R. Kearney, S. W. McKechnie, A. A. Hoffmann, *Science* **308**, 691 (2005).
- A. A. Hoffmann, C. M. Sgrò, *Nature* **470**, 479 (2011).
- S. Atwell *et al.*, *Nature* **465**, 627 (2010).
- J. Bergelson, F. Roux, *Nat. Rev. Genet.* **11**, 867 (2010).
- B. Brachi *et al.*, *PLoS Genet.* **6**, e1000940 (2010).
- C. Weinig *et al.*, *Genetics* **162**, 1875 (2002).
- D. H. Kim, M. R. Doyle, S. Sung, R. M. Amasino, *Annu. Rev. Cell Dev. Biol.* **25**, 277 (2009).
- B. Rathcke, E. P. Lacey, *Annu. Rev. Ecol. Syst.* **16**, 179 (1985).
- See supporting material in Science Online.
- A. M. Hancock *et al.*, *PLoS Genet.* **7**, e1001375 (2011).
- B. Charlesworth, M. T. Morgan, D. Charlesworth, *Genetics* **134**, 1289 (1993).
- J. H. Gillespie, *Genetics* **155**, 909 (2000).
- H.-u. -R. Athar, M. Ashraf, in *Handbook of Photosynthesis*, M. Pessarakli, Ed. (CRC Press, Boca Raton, FL, 2005), p. 928.
- H. A. Orr, *Evolution* **54**, 13 (2000).
- Z. Wang, B. Y. Liao, J. Zhang, *Proc. Natl. Acad. Sci. U.S.A.* **107**, 18034 (2010).
- G. P. Wagner, J. Zhang, *Nat. Rev. Genet.* **12**, 204 (2011).
- F. Roux, J. Gasquez, X. Reboud, *Genetics* **166**, 449 (2004).
- Z. Toomajian *et al.*, *PLoS Biol.* **4**, e137 (2006).

**Acknowledgments:** Funded by NIH GM083068 and NSF DEB0519961 to J.B. A.M.H. was supported by a V. Dropkin Postdoctoral Fellowship, and M.W.H. was

supported by an NSF Predoctoral Fellowship and a Graduate Assistance in Areas of National Need (GAANN) training grant. F.R. was supported by a Bonus Qualité Recherche (BQR) grant from the University of Lille, and B.B. received funding from a Ph.D. fellowship from the French Research Ministry and a mobility grant from the Collège Doctoral Européen. This is contribution 11-389-J from the Kansas Agricultural Experiment Station. We thank J. Borevitz, A. Fournier-Level, M. Nordborg, A. Platt, J. Schmitt, members of the Bergelson laboratory, and two anonymous reviewers for helpful input. Climate data for the 948 accessions used in these analyses, result files for the correlation analyses, and a browser that allows for viewing the results in their genomic context are available at <http://bergelson.uchicago.edu/regmap-data/> climate-genome-scan/. The genotype data used for these analyses resulted from the RegMap project (<http://regmap.uchicago.edu>).

## Supporting Online Material

[www.sciencemag.org/cgi/content/full/334/6052/83/DC1](http://www.sciencemag.org/cgi/content/full/334/6052/83/DC1)

Materials and Methods

Figs. S1 to S10

Table S1

References (23–35)

2 June 2011; accepted 25 August 2011

10.1126/science.1209244

# A Map of Local Adaptation in *Arabidopsis thaliana*

A. Fournier-Level,<sup>1</sup> A. Korte,<sup>2</sup> M. D. Cooper,<sup>1</sup> M. Nordborg,<sup>2</sup> J. Schmitt,<sup>1\*</sup> A. M. Wilczek<sup>1,3</sup>

Local adaptation is critical for species persistence in the face of rapid environmental change, but its genetic basis is not well understood. Growing the model plant *Arabidopsis thaliana* in field experiments in four sites across the species' native range, we identified candidate loci for local adaptation from a genome-wide association study of lifetime fitness in geographically diverse accessions. Fitness-associated loci exhibited both geographic and climatic signatures of local adaptation. Relative to genomic controls, high-fitness alleles were generally distributed closer to the site where they increased fitness, occupying specific and distinct climate spaces. Independent loci with different molecular functions contributed most strongly to fitness variation in each site. Independent local adaptation by distinct genetic mechanisms may facilitate a flexible evolutionary response to changing environment across a species range.

Adaptation to local environments has been observed experimentally in many organisms (1) and may critically limit a given species' capacity to evolve in the face of rapid environmental change (2–4). However, the molecular basis of local adaptation remains largely unexplored (5, 6). Understanding the genetic mechanisms of adaptation requires understanding the genetic basis of fitness variation within and across natural environments (7, 8). Although genome scans for signatures of past selection have identified candidate loci showing high levels of environmental differentiation

(9, 10), few studies have directly connected fitness variation measured in the natural environment of the species to the corresponding molecular variation (11, 12). Determining the extent of local adaptation requires identification of the loci associated with individual fitness in different natural environments, as well as characterization of the distribution pattern of adaptive variants, their environment specificity, and the type of genes involved.

To identify loci associated with fitness in the annual plant *Arabidopsis thaliana*, we grew a geographically diverse set of ecotypes (inbred lines derived from natural populations) across their native range, in replicated common garden experiments in four European field sites (fig. S1). Sites in Oulu (Finland) and Valencia (Spain) spanned the species climate range limits from Nordic to Mediterranean environments; sites in Halle (Germany) and Norwich (UK) represented

continental and oceanic climates at similar mid-range latitude (13). Mean survival and lifetime fruit (silique) production differed markedly among ecotypes within each planting site, indicating heritable variation among source populations in viability and fecundity (table S1). We carried out a genome-wide association study (GWAS) for survival and silique number using 213,248 single-nucleotide polymorphisms (SNPs) in a mixed-model approach to eliminate confounding due to genomic background (14, 15). For each fitness trait in each of the four field sites, we defined a set of associated SNPs corresponding to the 0.05% of the SNPs that explained the most variance (around 100 per GWAS; figs. S2 and S3). Individual SNPs explained a substantial amount of variation in lifetime fitness, with  $R^2$  in GWAS models ranging on average from 9% for the SNP set associated with survival in England to 24% for the SNP set associated with survival in Finland (fig. S1).

We tested whether alleles associated with high fitness in a given site were more locally abundant than genomic controls, as expected if they contributed to the local adaptation of that population (16). Indeed, the geographic centroids of the alleles associated with higher survival in England and Spain and silique number in Germany, England, and Spain were significantly closer to the planting sites in Germany, England, and Spain, respectively, relative to genomic controls; this constitutes evidence of local adaptation for specific loci (Fig. 1). Similar analyses excluding low-frequency polymorphisms provided similar results, demonstrating that the result was not biased as a result of the presence of rare alleles (table S2). In contrast, we found no evidence that the alleles conferring high fitness in Finland were locally abundant. However, our ability to detect

<sup>1</sup>Department of Ecology and Evolutionary Biology, Brown University, Providence, RI 02912, USA. <sup>2</sup>Gregor Mendel Institute, Austrian Academy of Sciences, 1030 Vienna, Austria. <sup>3</sup>Deep Springs College, Big Pine, CA 93513, USA.

\*To whom correspondence should be addressed. E-mail: johanna\_schmitt@brown.edu

## Adaptation to Climate Across the *Arabidopsis thaliana* Genome

Angela M. Hancock, Benjamin Brachi, Nathalie Faure, Matthew W. Horton, Lucien B. Jarymowycz, F. Gianluca Sperone, Chris Toomajian, Fabrice Roux and Joy Bergelson

*Science* **334** (6052), 83-86.  
DOI: 10.1126/science.1209244

### ARTICLE TOOLS

<http://science.sciencemag.org/content/334/6052/83>

### SUPPLEMENTARY MATERIALS

<http://science.sciencemag.org/content/suppl/2011/10/05/334.6052.83.DC1>

### RELATED CONTENT

<http://science.sciencemag.org/content/sci/334/6052/11.1.full>  
<http://science.sciencemag.org/content/sci/334/6052/49.full>

### REFERENCES

This article cites 31 articles, 14 of which you can access for free  
<http://science.sciencemag.org/content/334/6052/83#BIBL>

### PERMISSIONS

<http://www.sciencemag.org/help/reprints-and-permissions>

Use of this article is subject to the [Terms of Service](#)